

CERN-EP/82-84  
25 June 1982SEARCH FOR NARROW  $\bar{p}p$  STATES IN BARYON EXCHANGE REACTIONSCERN<sup>1</sup>-Neuchâtel<sup>2</sup>-Palaiseau(Ec.Poly.)<sup>3</sup>-Paris(Coll. de France)<sup>4</sup> Collaboration

Z. Ajaltouni<sup>3</sup>, L. Bachman<sup>2</sup>, A. de Bellefon<sup>4</sup>, P. Benkheiri<sup>3</sup>, P. Billoir<sup>4</sup>,  
 M. Bogdanski<sup>2+</sup>, J.M. Brunet<sup>4</sup>, B. Chaurand<sup>3</sup>, L. Dorsaz<sup>2</sup>, A. Ferrer<sup>1\*</sup>,  
 L. Fluri<sup>2</sup>, P. Frenkiel<sup>4</sup>, J.M. Gago<sup>1\*\*</sup>, B. Lefièvre<sup>4</sup>,  
 D. Perrin<sup>2</sup>, D. Poutot<sup>4</sup>, A. Rougé<sup>3</sup>, P. Sonderegger<sup>1</sup>, P. Triscos<sup>4</sup>,  
 G. Tristram<sup>4</sup>, A. Volte<sup>4</sup> and J.P. Wuthrick<sup>3</sup>

ABSTRACT

The results of a search for narrow  $\bar{p}p$  states produced backwards in the baryon exchange reactions  $\pi^- p \rightarrow \Delta_f^0(1232)\bar{p}p$  and  $\pi^- p \rightarrow N_f^0(1520)\bar{p}p$  at 12 GeV/c and  $\pi^+ p \rightarrow \Delta_f^{++}(1232)\bar{p}p$  at 20 GeV/c, are reported. No structures of statistical significance exceeding three standard deviations have been found in the  $\bar{p}p$  mass spectra. Limits on the cross-sections are given and compared with previous results.

(Submitted to Physics Letters)

- 
- + Now at Laboratoire Suisse de Recherches Horlogères, Neuchâtel.
  - \* On leave of absence from: LAL, Orsay, France.
  - \*\* On leave of absence from: Inst. Nac. de Invest. Cientifica, Lisbon, Portugal.

Two narrow  $\bar{p}p$  peaks of invariant masses 2020 and 2200 MeV/c<sup>2</sup> were reported in 1977 by Benkheiri et al.<sup>1)</sup> in the baryon exchange reaction

$$\pi^- p \rightarrow p_f \pi^- \bar{p}p \text{ at 9 and 12 GeV/c}$$

where the system of the forward produced  $p_f$  and the  $\pi^-$  is either in the  $\Delta^0(1232)$  or in the  $N^0(1520)$  band.

In an attempt to confirm these peaks, we have used the data of an experiment originally designed for a high sensitivity search for doubly charged exotic mesons produced via baryon exchange in  $\pi^+p$  interactions at 20 GeV/c. A preliminary analysis of the four-prong reaction  $\pi^- p \rightarrow p_f \pi^+ \bar{p}p$  without neutrals based on 20% of the presently available statistics showed no enhancement at 2020 and a small 2 s.d. effect at 2200 MeV/c<sup>2</sup><sup>2)</sup>.

Several other experiments<sup>3-6)</sup> have recently reported negative results on the existence of these structures, in various baryon exchange reactions. Also, and in order to reproduce more closely the experimental conditions of Ref. 1, we have taken data with a  $\pi^-$  beam at 12 GeV/c (the higher of the two momenta used in Ref. 1).

We report hereafter final results for the  $p_f \pi^\pm$  and the  $\bar{p}p_s$  spectra observed in the reactions

$$\pi^- p \rightarrow p_f \pi^- \bar{p}p_s \text{ at 12 GeV/c} \quad (1)$$

$$\pi^+ p \rightarrow p_f \pi^+ \bar{p}p_s \text{ at 20 GeV/c} \quad (2)$$

The experiment was done in the newly upgraded Omega spectrometer<sup>7)</sup> at the CERN SPS, with proportional chambers inside the magnet and drift chambers at its downstream end replacing the optical chambers used for the experiment of Ref. 1. The incident particles were identified by a CEDAR Čerenkov counter and their momenta and angles measured by a scintillation counter hodoscope and a set of seven MWPCs of 1 mm pitch. The 60 cm long hydrogen target was surrounded by a 24-element scintillation hodoscope ("barrel") and a  $1/2$  mm pitch wire chamber at its downstream end (Y1 in Fig. 1) which together provided a measurement of the charged multiplicity. A set of 32 MWPC planes (type C) and of 30 forward MWPC planes (type B and A in Fig. 1) were used to reconstruct the out-going particles. The

magnetic field in the detector volume was 1.8 Tesla. Two drift chambers (DC1 and DC2) were used to improve the measurement accuracy for fast particles.

The main trigger requirement was the detection of a fast forward produced particle of momentum greater than half the beam momentum, and which did not give light in either of the two multicell atmospheric Čerenkovs  $\check{C}_1$  and  $\check{C}_2$  filled with Freon-114 and  $N_2$ , respectively. The new MBNIM modules<sup>8)</sup> were used to discard the events which did not satisfy the appropriate correlations between hodoscopes H2 and H3 and the two Čerenkov counters. Other MBNIM modules computed the momentum of the trigger particle from three proportional planes (Y0, Y3 and Y4 in Fig. 1) and provided a rather sharp momentum cut. Several multiplicity requirements were imposed:  $\geq 1$  in the barrel hodoscope,  $\geq 1$  in Y1,  $\geq 3$  in the two of them, 2 to 5 in Y2 and  $\leq 3$  in Y3. A  $\gamma$ -veto consisting of hodoscopes H3 and H4 and a lead sheet of 15 mm thickness in between, eliminated events with fast  $\pi^0$ 's.

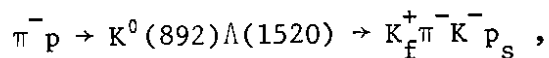
All the triggers have been processed through the TRIDENT<sup>9)</sup> program, developed at CERN. It reconstructs the tracks geometrically, taking into account the  $\Omega$  magnetic field map, and finds the interaction vertex. We then selected four-prong charge-balanced events, with a vertex inside the hydrogen target. Only events with a fast proton momentum  $> 10$  GeV/c ( $\pi^+$  run) and  $> 7$  GeV/c ( $\pi^-$  run) and which satisfy  $|u|^* < 1.6$  (GeV/c<sup>2</sup>)<sup>2</sup>, were retained for further analysis. These events were processed through a vertex-fit program, developed for this experiment, that constrained all the tracks to pass through the same vertex point<sup>10)</sup>. Finally, 4 constraint kinematical fits were performed using the modified program KOMEGA<sup>11)</sup>. These reject completely the triggers due to fast K<sup>+</sup>'s. (The few K<sup>+</sup> triggers found in the  $\pi^+$ p events are attributed to a local inefficiency of Čerenkov  $\check{C}_1$  in the median plane; for the  $\pi^-$ p events, the majority (70%) of the triggers were due to K<sup>+</sup>'s of momenta near and below 9.6 GeV/c, the threshold of  $\check{C}_1$  for K's.)

Table 1 gives for the two reactions (1) and (2), the total number of triggers, the corresponding beam fluxes, and the numbers of events of the two four-body reactions (1) and (2) identified with a  $\chi^2$  probability  $\geq 4\%$ .

---

\*)  $u$  is the four momentum transfer squared from the incident  $\pi$  to the outgoing fast proton.

The momentum imbalance distributions  $\vec{p}_{inc} - \vec{\Sigma p}_{out}$  of these events show standard deviations of  $\pm 65$  MeV/c in the beam direction and  $\pm 22$  MeV/c in the transversal directions. These values are slightly better than those obtained in the spark chamber experiment of Ref. 1. Momenta are measured to  $\pm 1\%$  for the incident particle,  $\pm 3$  to  $5\%$  for the fast proton, and  $\sim \pm 1\%$  for the slow tracks. The resulting invariant mass measurements are quite accurate before any fit: we find  $\Delta M = \pm 2$  and  $7$  MeV/c<sup>2</sup> for  $\Lambda$ 's and  $K^0$ 's of momenta  $\leq 3$  GeV/c obtained in this experiment. The final mass resolution (after kinematical fitting) for the  $\bar{p}p_s$  system in reactions (1) and (2) is  $\sigma_M = 2.0$  MeV/c<sup>2</sup> at  $M_{\bar{p}p} = 2020$  MeV/c<sup>2</sup>, and  $\sigma_M = 3.8$  MeV/c<sup>2</sup> at  $M_{\bar{p}p} = 2200$  MeV/c<sup>2</sup>. These values were deduced from a careful study of the reaction



which was measured in the same experiment. The backwards produced  $\Lambda(1520) \rightarrow p_s K^-$  is very narrow and the kinematical properties are similar to reaction (1). Unfolding the intrinsic width of  $15.5$  MeV/c<sup>2</sup> from the experimentally measured  $\Gamma = 19$  MeV, we found  $\sigma_\Lambda = 4$  MeV/c<sup>2</sup>. The TRIDENT errors were consequently scaled up and the above values for reactions (1) and (2) obtained.

We show in Fig. 2 the results obtained in the analysis of the  $\pi^-$  data, and in Fig. 3 those of the  $\pi^+$  data.

Figures 2a and 2b show the  $p_f \pi^-$  and  $\bar{p}p_s$  effective masses for the whole sample of  $\pi^-$  data at  $12$  GeV/c. Only the  $N_{fast}^{*0}(1520)$  baryon seems to be clearly present in our data. A weak "shoulder" at the  $\Delta^0(1232)$  mass appears, especially when one selects events with  $\bar{p}p$  masses  $< 2.2$  GeV/c<sup>2</sup> (hatched curve in Fig. 2a). No indication of bumps is present in the  $\bar{p}p$  mass spectra. Despite the absence of a clear  $\Delta_{fast}^0(1232)$  signal, we have selected the events according to the cuts used in Ref. 1. We define two samples of data:  $\Delta^0(1232)$  selection ( $1.10 \leq m_{p\pi} \leq 1.30$  GeV/c<sup>2</sup>) and  $N^{*0}(1520)$  selection ( $1.45 \leq m_{p\pi} \leq 1.60$  GeV/c<sup>2</sup>). For both samples, we display the  $p_s \bar{p}$  mass spectra in Figs. 2c and 2d, respectively. The hatched spectra drawn in the  $p_s \bar{p}$  mass distributions correspond to  $\cos \theta_J(\bar{p}) < 0$  cut, where  $\theta_J$  is the Jackson decay angle of the  $\bar{p}$  in the  $p_s \bar{p}$  rest system. This cut reduces

the contribution of the (dominant) diffractive mechanism which is characterized by a slow  $p_s$  in the laboratory system (slower than the  $\bar{p}$ ). No bumps are observed in any of these spectra.

Figures 3a and 3b show the  $p_f \pi^+$  and  $\bar{p} p_s$  masses for the complete 20 GeV/c  $\pi^+$  data. In contrast to the  $\pi^- p$  reaction, a strong  $\Delta_{fast}^{++}$  (1232) production is observed. A  $\Delta_{slow}^{++}$  (1232) is found in the  $p_s \pi^+$  spectrum, with twice as many events as in the  $\Delta_{fast}^{++}$  (1232) peak, and indicates a non-baryon exchange production mechanism. We have removed the events with the  $p_s \pi^+$  system in the  $\Delta$ (1232) region from our sample. The resulting hatched spectrum in Fig. 3a shows that the  $\Delta_{fast}^{++}$  (1232) events are not affected by this cut. Figure 3c shows the  $\bar{p} p_s$  effective mass distribution for events with  $\cos \theta_J(\bar{p}) \leq 0$ , which again eliminates most of the diffractive background. Once more, no bumps at 2020 or 2200 MeV/c<sup>2</sup> are seen.

To estimate cross sections we have computed the effective total interaction rate for  $\pi^-$  and  $\pi^+$  data (63 reactions/nb and 427 reactions/nb, respectively), the geometrical acceptance of the apparatus and the losses due to our selection criteria. The trigger and counter efficiencies were measured. A quasi two-body Monte Carlo simulation program generated events and tracked them through the whole apparatus, in order to assess the pattern recognition and vertex finding efficiency. The losses due to absorption of particles in the target and detectors were also included in the acceptance calculations. Details are given in Ref. 12.

Some well-known reactions were also measured in this experiment and were used as a cross-check for the acceptance calculations, namely the backward elastic and backward  $\rho^-$  production reactions in the  $\pi^-$  data [ $\pi^- p \rightarrow p_f \pi^-$  (13) and  $\pi^- p \rightarrow p_f \rho^-$  (14)] and reaction  $pp \rightarrow \Delta^{++}(1232)n$  for the  $\pi^+$  sample (15).

The total acceptance is almost constant for  $\bar{p} p_s$  masses from threshold to 2200 MeV/c<sup>2</sup>, and is  $\sim 6\%$  for  $\pi^- p \rightarrow \Delta_f^0(1232)\bar{p} p_s$ , 4% for  $\pi^- p \rightarrow N^0(1520)\bar{p} p_s$ , and 7% for  $\pi^+ p \rightarrow \Delta_f^{++}(1232)\bar{p} p_s$ . This gives a sensitivity of 3.7 and 2.5 fitted events per nanobarn for the two  $\pi^- p$  reactions, roughly a factor of two above the sensitivity of Ref. 1. and a factor of two below the sensitivity of Ref. 4. For the  $\pi^+ p$  reaction, a sensitivity of 30 fitted events per nanobarn results, well above the figures reached so far in reactions of this type.

Taking into account the mass resolutions given above, we report in Table 1 the 99.8% C.L. upper limit for the cross sections for backward production of narrow  $\bar{p}p_s$  states, in both  $\pi^-p$  and  $\pi^+p$  reactions under the assumption of isotropic decay in the  $\bar{p}p_s$  rest systems.

In conclusion, from a study of the reactions  $\pi^-p \rightarrow p_f \pi^- \bar{p}p$  at 12 GeV/c, and  $\pi^+p \rightarrow p_f \pi^+ p\bar{p}$  at 20 GeV/c, we do not find evidence for any narrow  $\bar{p}p$  structure produced backwards, for example, via a baryon exchange mechanism. Our results do not confirm, in particular, the evidence for the narrow peaks at 2020 MeV/c<sup>2</sup> and 2200 MeV/c<sup>2</sup> reported by Benkheiri et al.<sup>1)</sup>, despite the fact that the  $\pi^-$  data sample has been taken at one of the beam energies used in Ref. 1. The cross section limits obtained are three to five times lower than the cross sections of Ref. 1, depending on the channel.

REFERENCES

- 1) P. Benkheiri et al., Phys. Lett. 68B (1977) 483; Phys. Lett. 81B (1979) 380.
- 2) A. Ferrer, Review of  $\bar{p}p$  production experiments at CERN, AIP Conf. Proc. 67 (1981) 123.
- 3) R.M. Bionta et al., Phys. Rev. Lett. 44 (1980) 909.
- 4) S.U. Chung et al., Phys. Rev. Lett. 20 (1980) 1611.
- 5) T. Armstrong et al., Preprint INFN-BA-OM 81-02 (November 1981).
- 6) C. Evangelista et al., Nucl. Phys. B184 (1981) 189.
- 7) W. Beusch, The Omega Prime Project, CERN-SPSC/77-70/T17.
- 8) A. Corre et al., Nucl. Instrum. Methods 179 (1981) 585.
- 9) J.-C. Lassalle, F. Carena and S. Pensotti, TRIDENT, track and vertex identification program for the Omega particle detector system, CERN-DD/EE/79-2.  
J.-C. Lassalle et al., Nucl. Instrum. Methods 176 (1980) 371.
- 10) P. Billoir, Ph.D. Thesis, to be published.
- 11) KOMEGA, CERN Program Library; and P. Benkheiri, Ph.D. Thesis.
- 12) Z. Ajaltouni, Thèse 3<sup>e</sup> cycle, Orsay no. 3053 (LPNHE/X/81, July 1981).
- 13) A. Jacholkowski et al., Nucl. Phys. B126 (1977) 1.
- 14) P. Benkheiri et al., Lett. al Nuovo Cimento 20 (1977) 297.
- 15) H. Bøggild et al., Phys. Lett. 30B (1969) 369.

Table 1

	$\pi^-$ (12 GeV/c)		$\pi^+$ (20 GeV/c)	
Total number of triggers	$2.6 \times 10^6$		$8.6 \times 10^6$	
Total incident flux	$31.5 \times 10^9$ (63 ev./nb)		$18.8 \times 10^{10}$ (427 ev./nb)	
Total number of 4C-fits:	13100		36845	
$M_{\bar{p}p}$ (MeV/c <sup>2</sup> )	2020	2200	2020	2200
99.8% CL				
Cross section upper limits				
$\Delta(1232)M_{\bar{p}p}$	2 nb	3 nb	1 nb	1.5 nb
$N^0(1520)M_{\bar{p}p}$	6 nb	8 nb	-	-



Figure captions

- Fig. 1 : The Omega Spectrometer layout for this experiment (WA56), see text. The time of flight counter (TOF) was not used for the results presented here.
- Fig. 2 : a)  $p_f \pi^-$  effective mass. All data (13100 events). Hatched curve, events with  $\bar{p}p$  mass  $< 2.2 \text{ GeV}/c^2$  only.  
b)  $\bar{p}p_s$  effective mass, all data. Hatched curve, events with  $\cos \theta_J(\bar{p}) < 0$  only (1088 events).  
c)  $\bar{p}p_s$  effective mass, events in the  $\Delta^0(1232)$  region -- see text -- Hatched curve, events with  $\cos \theta_J(\bar{p}) < 0$  only (168 events).  
d)  $\bar{p}p_s$  effective mass, events in the  $N^0(1520)$  region. Hatched curve, events with  $\cos \theta_J(\bar{p}) < 0$  only (335 events).
- Fig. 3 : Results from  $\pi^+ p \rightarrow p_f \pi^+ p_s \bar{p}$  reaction at 20 GeV/c.  
a)  $p_f \pi^+$  effective mass. All data (36845 events). Hatched curve, events with  $\Delta_{\text{slow}}^{++}(1232)$  subtracted.  
b)  $\bar{p}p_s$  effective mass, all data. Hatched curve, events with  $\cos \theta_J(\bar{p}) < 0.0$  only (3917 events).  
c)  $\bar{p}p_s$  effective mass, events in the  $\Delta_f^{++}(1232)$  region (see text). Hatched curve, events with  $\cos \theta_J(\bar{p}) < 0$  only (776 events).

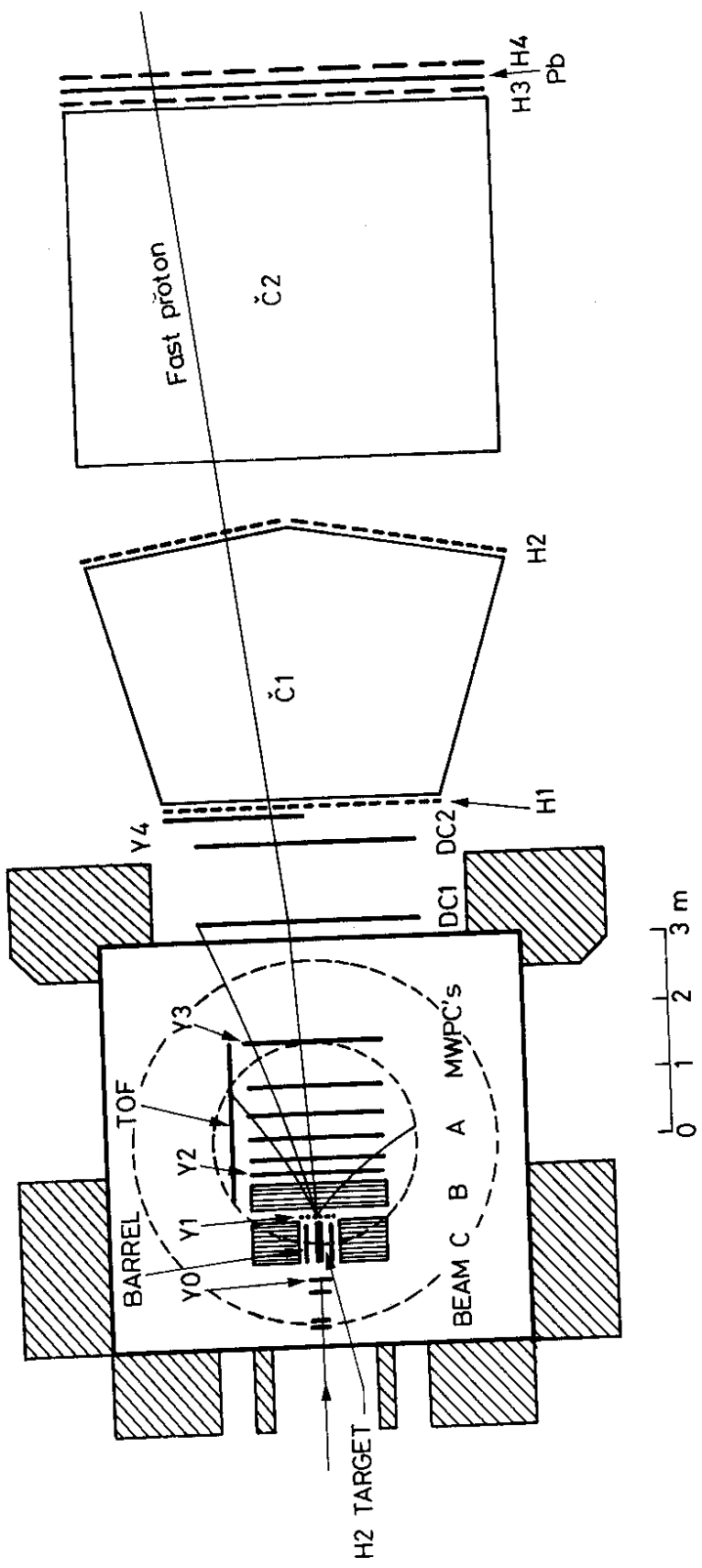


Fig. 1

$\pi^- p \rightarrow p_f \pi^- p_s \bar{p}$  at 12 GeV/c

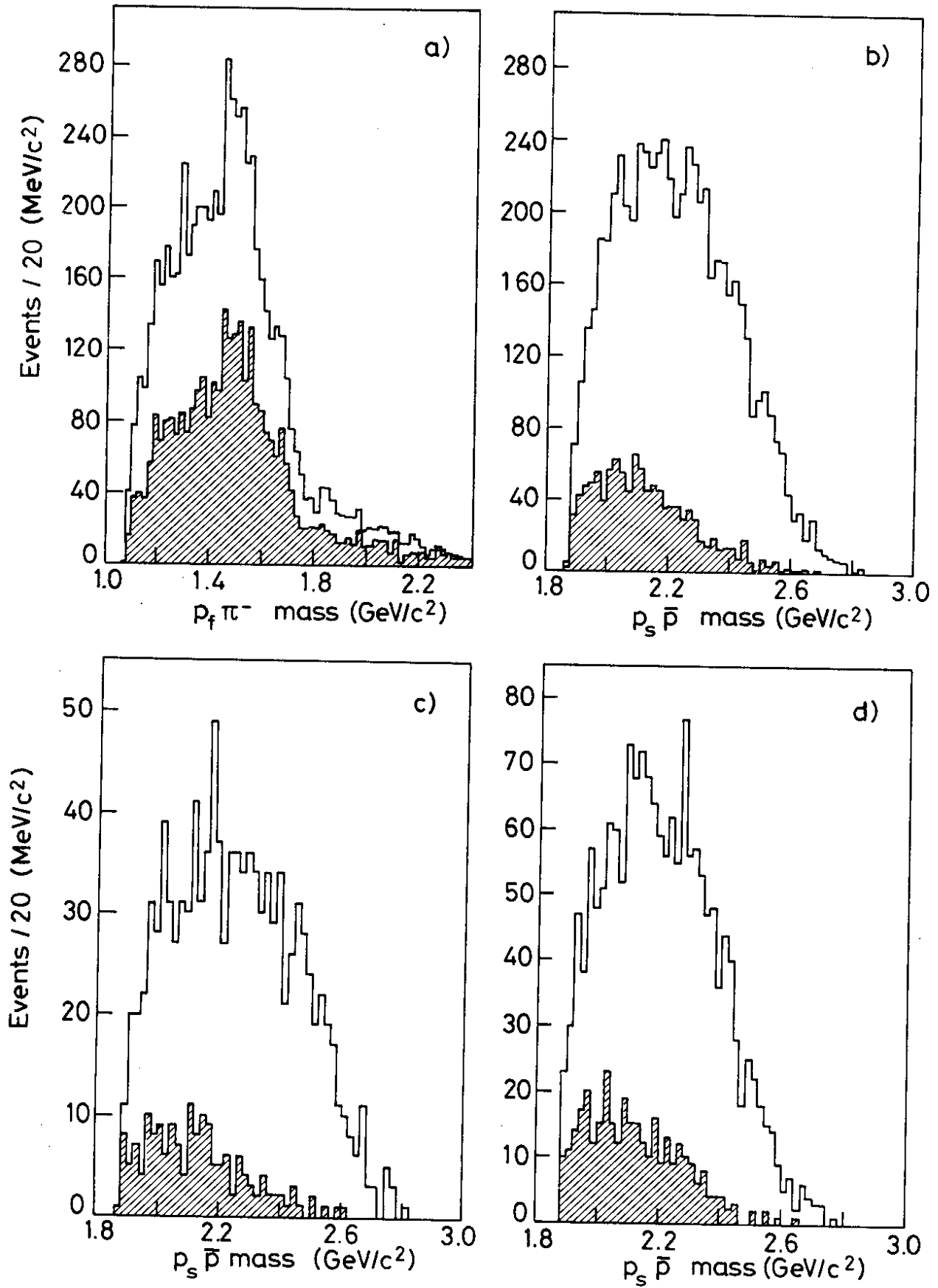


Fig. 2

$\pi^+ p \rightarrow p_f \pi^+ p_s \bar{p}$  at 20 GeV/c

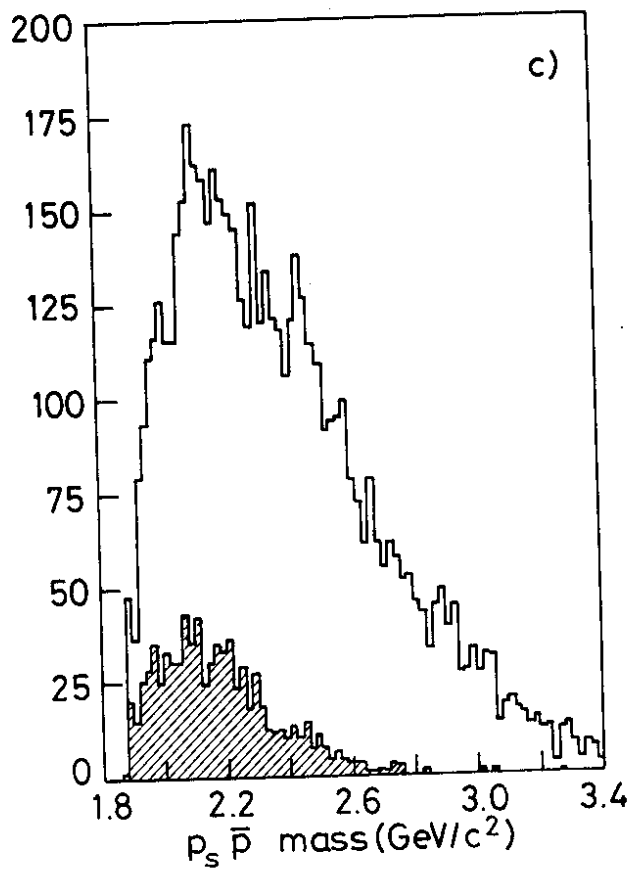
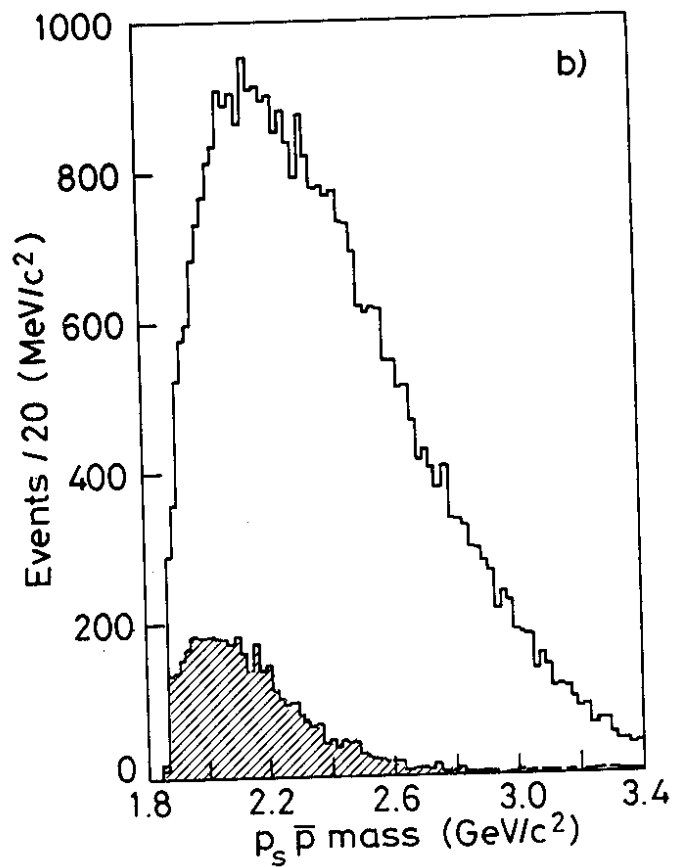
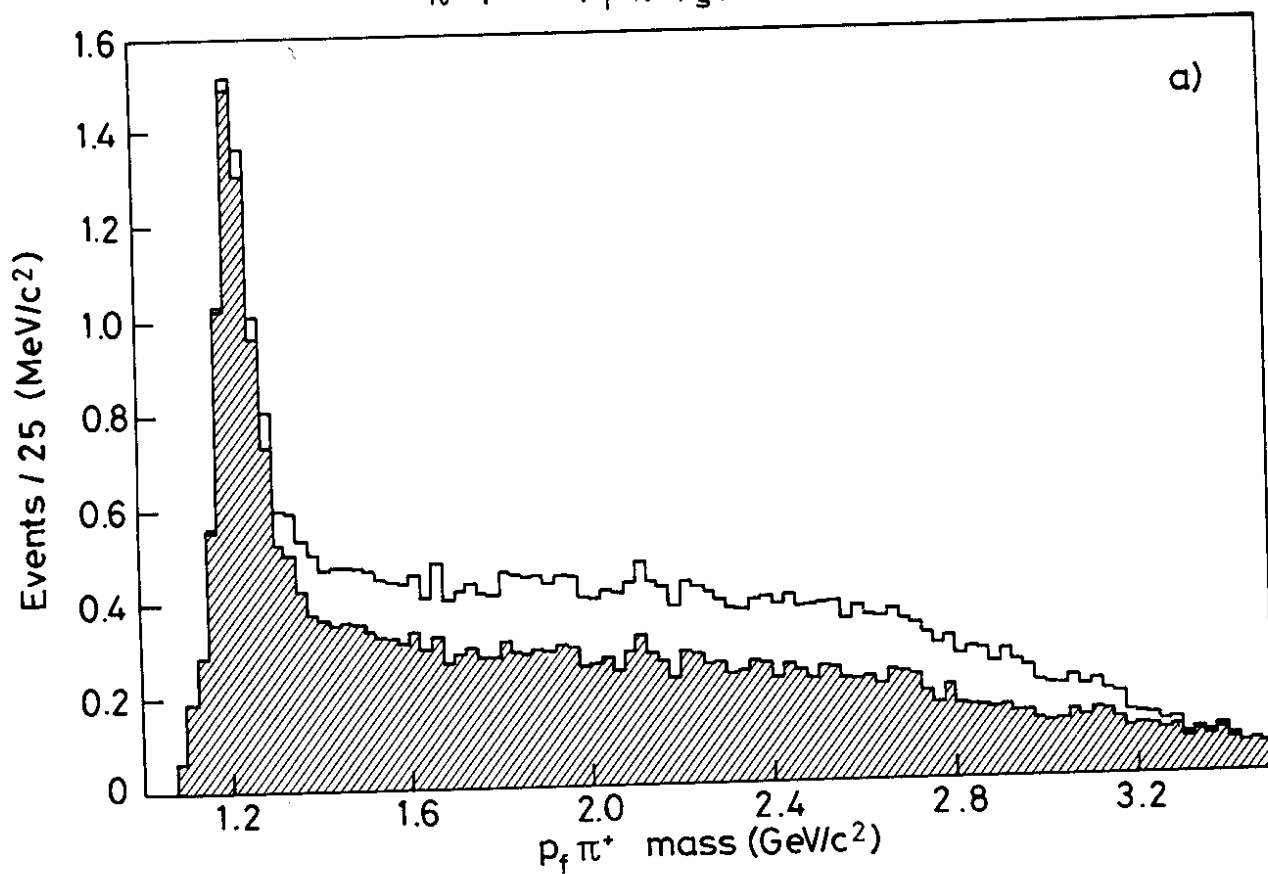


Fig. 3

